Recent Advances in Perovskite-Based Building-Integrated Photovoltaics

Recent Advances in Perovskite-based Building-Integrated Photovoltaics

Munkhbayar Batmunkh, Yu Lin Zhong and Huijun Zhao**

Dr. M. Batmunkh, A/Prof. Y. L. Zhong, Prof. H. Zhao
Centre for Clean Environment and Energy
School of Environment and Science
Griffith University
Gold Coast, Queensland 4222
Australia
E-mail: y.zhong@griffith.edu. au; h.zhao@griffith.edu. au

Keywords: building-integrated photovoltaics, solar windows, smart windows, solar harvesting materials, perovskite

Perovskite-based solar cells have attracted great attention due to their low cost and high photovoltaic (PV) performance. In addition to their success in the PV sector, there has been growing interest in employing perovskites in energy-efficient smart windows and other building technologies owing to their large absorption coefficient and color tunability. The major challenge lies in integrating perovskite materials into windows and building facades and combining them with added functionalities while maintaining their remarkable power conversion efficiencies. This Progress Report highlights advances that have been made in the application of perovskites to building-integrated photovoltaics (BIPVs) in four areas: semitransparent windows, colorful wall facades, electrochromic windows, and thermochromic windows. In addition, the opportunities and challenges of this cutting-edge research area and important roadmaps for the future use of perovskites in BIPVs are discussed.

1. Introduction

Perovskites are excellent solar harvesting materials and have gained a great deal of attention from the photovoltaic (PV) community over the past ten years.[1] In 2009, Miyasaka and his colleagues first reported on organic–inorganic lead halide perovskite semiconductors as active light absorbers in solar cells.[2] In this pioneering work, the best performing device delivered a power conversion efficiency (PCE) of 3.8% and was stable for only a few minutes. Despite

this, several research groups in the PV field have paid further attention to the development of perovskite-based solar cells.[3-5] Researchers found that perovskite light absorbers exhibit promising photovoltaic properties, such as tunable bandgaps, high absorption coefficients, high charge carrier mobility, and long charge diffusion lengths.[6-8] In mid-2012, a collaborative publication by Grätzel and Park reported solid-state perovskite PV devices with a PCE of 9.7%.[9] Later in the same year, Snaith and co-workers demonstrated that perovskites are not only efficient light absorbers, but also facilitate the transport of photogenerated charges to electrodes, obtaining 10.9% efficiency.[10] This was the pivotal moment when perovskite solar cells (PSCs) became the front runner among emerging PVs, and the field has advanced dramatically ever since. PV devices made from perovskite materials can now produce PCEs comparable to those of silicon solar cells (both converting ~25% of solar energy into electricity).[11]

In addition to traditional roof-top solar panels, building-integrated photovoltaics (BIPVs) have been recognized as a pivotal technology that enables the innovative utilization of renewable solar energy on other building areas, such as windows and exterior walls.[12] This allows for a large surface area of the building to be used for solar harvesting.[13] To this end, perovskite materials are highly promising because of their low production cost, facile processability, and color tunability.[14] For instance, high-efficiency PSCs (~20%) can now be fabricated in the form of thin flexible films,[15] which are very promising for the effective utilization of building rooftops (Figure 1). Furthermore, a wide range of added functionalities, such as light and heat modulation, will allow for high overall energy-saving efficiency.

Perovskite-based BIPVs have undergone considerable development over the past few years and can be categorized according to their functionalities. The most widely explored type is the semitransparent perovskite solar cell (ST PSC), which can be directly applied to building facades, windows, and glass roofs for solar harvesting.[16] Major advancements have been made in the development of these PSCs, and there are several reviews providing a broad

perspective of this field.[16-19] A more recent review, highlighting the current advances, was conducted by Shi *et al*.[20] Colorful PSCs are an attractive type of BIPV that show promising applicability to building walls, fences, and parking roofs.[21] A more challenging type of BIPV combines the solar harvesting function with an electrochromic layer, forming dual-function photovoltachromic cells (PVCCs).[22-27] The same combination can be used for thermochromic and light-harvesting materials to yield a thermochromic solar cell.[28-31] The main motivation for these dual-functional BIPVs is to create smart windows that can help to cool buildings by shading out sunlight and harvesting it to generate electricity in the hot summer sun.[32]

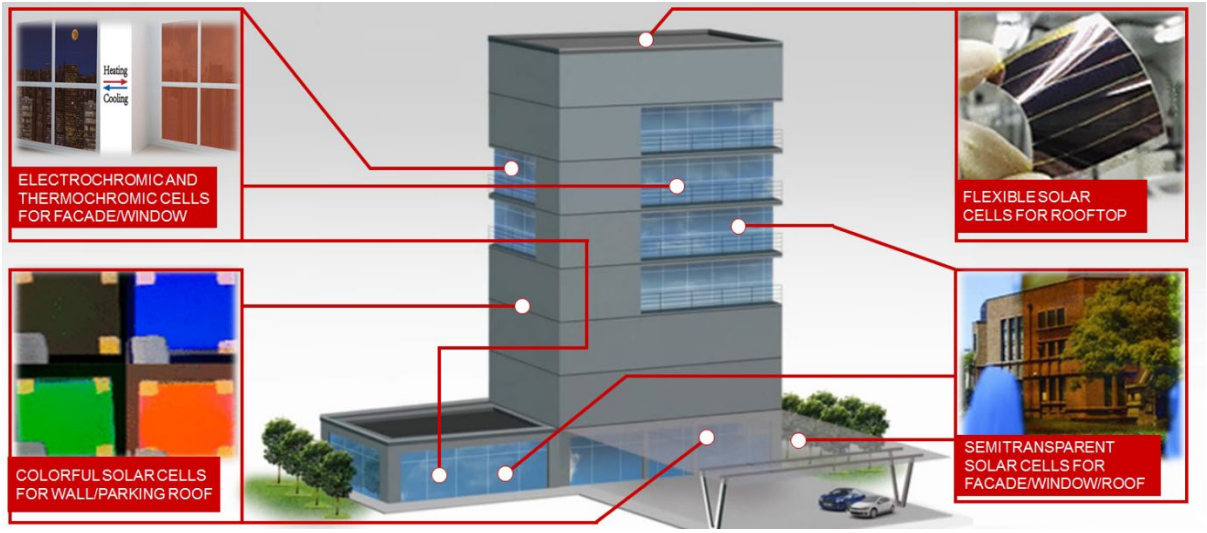

Figure 1. The wide applicability of perovskite-based BIPVs. Note: while the most effective uses of each type of solar cell are suggested, there are many other applications. For instance, ST PSCs can be applied on facades, windows, and glass roofs, while colorful solar cells can also be installed on walls, windows, and roofs. Electrochromic and thermochromic solar cells are suitable for windows, facades, and parking roofs. The building architecture was reproduced from ref. [33]. ST PSC was reproduced with permission.[34] Copyright 2016, WILEY-VCH. Colorful PSCs were obtained with permission.[21] Copyright 2019, American Chemical Society. The flexible PSC was reproduced with permission.[35] Copyright 2018, American Chemical Society. Electrochromic solar cells were reproduced with permission.[23] Copyright 2019, WILEY-VCH.

In this progress report, we first highlight the recent advancements in ST PSCs and colorful PSCs, and then examine the notable achievements made with perovskite-based PVCCs and thermochromic solar cells (see Figure 1). Although excellent progress has been made within a short period of time, research into perovskite-based BIPVs is still in its early stages. Hence, this Progress Report will offer critical roadmaps for future developments of perovskite-based BIPVs to eventualize their large-scale commercialization.

2. Semitransparent PSCs

Semitransparent photovoltaic (ST PV) cells have received significant attention for integration into buildings. Unlike silicon solar cells, which are mostly limited to rooftop or field applications, ST PV cells are suitable for windows and glass roofs. The incident heat gain into buildings can be reduced by partially blocking (or absorbing) sunlight with ST PV windows, and using it to generate electricity.[20] An ideal ST solar cell for integration into buildings should exhibit high PV efficiency and excellent optical properties such as high average visible transmittance (AVT), color rendering index (CRI), and average near-infrared (NIR) transmittance.[17] However, there is a significant trade-off between PCE and transmittance in ST solar cells. Owing to their large absorption coefficient and tunable bandgap, perovskite-based devices have shown great promise as ST solar cells for BIPVs.[16, 17, 20] Recently, Shi et al.[20] summarized the advancements in the fabrication of ST PSCs. In this section, after providing a brief overview of ST PSCs, we discuss their critical integration into building applications.

High-efficiency PSCs strongly rely on uniform, pinhole-free perovskite films with thicknesses ranging from 300 to 400 nm (in order to make the films opaque).[36-38] Therefore, a simple strategy to increase the light transmittance of devices is to reduce the thickness of the perovskite layer.[34, 39-41] For instance, Carmona et al. fabricated inverted PSCs with perovskite thicknesses of 180 nm and 100 nm, and obtained PCEs of 7.3% and 6.4% with

AVTs of 22% and 29%, respectively.[39] Subsequently, Qi's group reported $CH_3NH_3PbI_{3-x}Cl_x$-based n-i-p structured PSCs and achieved an efficiency of 9.9% using a device with a 135 nm perovskite film.[40] Furthermore, by using a 180-nm-thick perovskite film, an inverted device (ST PSC) with an AVT of approximately 25% delivered a PCE of more than 10%.[42] This ST PSC was assembled on a highly transparent CuSCN-coated indium-doped tin oxide (ITO) glass substrate. The optical transparency of the thin CuSCN film was over 90% in the wavelength range of 350 – 1100 nm.

In general, neutral-colored ST solar cells are appealing for window applications, but the perovskite films are typically reddish brown or dark brown.[16] Snaith's group demonstrated a de-wetting strategy to prepare island-structured perovskite with incomplete coverage, to obtain a neutral-colored perovskite film.[43] The film transmittance was adjusted by changing the coverage of the perovskite. The fabricated ST PSCs, with a thin gold electrode (10 nm), displayed PCEs of 8–3.5% at AVTs of 7–30%. The same authors also demonstrated a neutral-colored, microstructured formamidinium lead iodide ($FAPbI_3$) perovskite-based ST-PSC that used a transparent conductive electrode based on a novel nickel mesh.[44] The ST PSC device showed a promising PCE of 5.2% at an AVT of 28%.

In this class of PSCs, one critical issue is the direct contact of electron- and hole-transporting layers in the perovskite-free region (Figure 2a), resulting in poor PCEs. Hörantner et al.[45] attempted to address this issue by applying a shunt-blocking layer (alkyl–siloxane) to the uncovered surface of the electron-collecting layer. This transparent, insulating molecular layer was found to be effective in reducing the charge recombination rates. As a result, a PCE of 6.1% was obtained for a neutral-colored ST PSC with 38% AVT. A polystyrene insulator was also used as a passivation layer to increase the shunt resistance of perovskite islands based on ST solar cells (Figure 2b and 2c).[46]

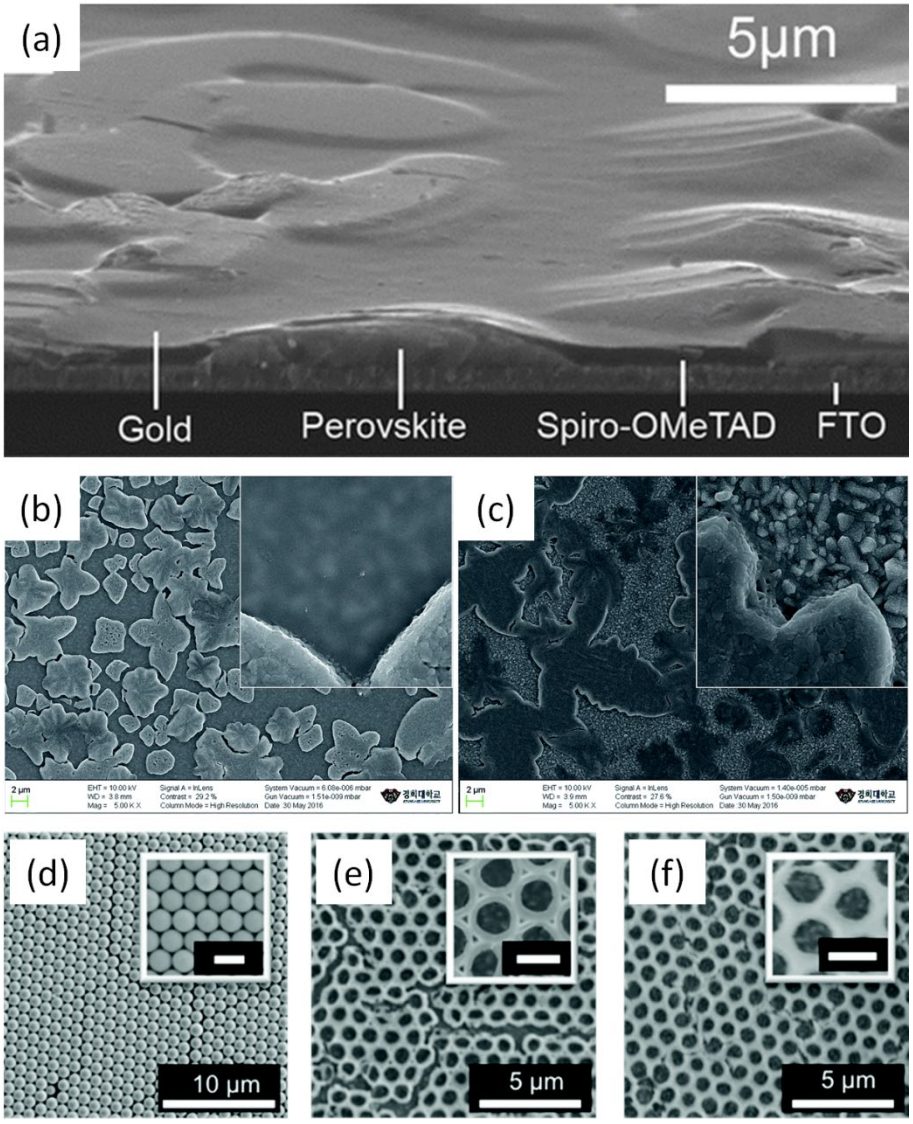

Figure 2. (a) Cross-sectional scanning electron microscopy (SEM) image of an ST PSC prepared using a de-wetting strategy. Reproduced with permission.[43] Copyright 2014, American Chemical Society. (b) Top-view SEM images of $MAPbI_3$ islands/TiO_2/FTO substrates (b) with and (c) without a polystyrene passivation layer. Reproduced with permission.[46] Copyright 2016, The Royal Society of Chemistry. SEM images (with magnified insets, scale bar 1 μm) showing (d) a typical highly ordered monolayer of 1 μm diameter polystyrene microspheres, (e) cured TiO_2, and (f) SiO_2 honeycomb structure. Reproduced with permission.[47] Copyright 2015, The Royal Society of Chemistry.

In addition, controlling the microstructure of perovskite is a promising method for realizing ST PSCs.[48] For example, Snaith's group controlled the domain size and microstructure of the perovskite by guiding crystal growth using a highly ordered metal oxide honeycomb structure

(Figure 2d-f).[47] The perovskite fills the holes of the honeycomb, where the honeycomb region is transparent. ST PSCs fabricated using such structures achieved a PCE of up to 9.5% with an AVT of approximately 37%. In another example, Moon et al.[49] prepared parallel aluminum oxide nanopillars as a scaffold layer to obtain nanostructured perovskites for ST PSC fabrication (Figure 3a). The transmittance of the device was controlled by the thickness of the perovskite layer (Figure 3a). A PCE of 9.6% with an AVT of 33.4% was achieved for the optimized device. Since structural control over perovskite layers is a promising strategy for ST PSCs, more attention should be paid to the development of a novel design for perovskite growth. Some well-established methods for accurately controlling the perovskite growth, such as etching and effective deposition, should be explored for the fabrication of ST PSCs.

A typical PSC is fabricated with a metal electrode on the surface that is made from gold (Au) or silver (Ag) and serves as a current collector. However, a thick opaque metal layer is undesirable for ST PSCs. Carmona et al.[39] reported that a 100 nm layer of LiF could serve as a capping layer on an ultrathin (only 6 mm) Au electrode. The use of LiF not only improved the efficiency of the ST PSCs, but also enhanced the device transparency (Figure 3b). Gaspera et al.[50] designed a multilayered dielectric–metal–dielectric (DMD) (MoO_3–Au–MoO_3) electrode for PSCs using thermal evaporation. A DMD electrode with 5 nm of MoO_3 on the bottom, 10 nm of Au in the middle, and 35 nm of MoO_3 on top, resulted in the highest PCE of 13.6%, but the corresponding AVT was only 7%.

Transparent conductive electrodes (TCEs), based on nanocarbons such as carbon nanotubes (CNTs) and graphene, are promising candidates for ST PSCs owing to their high conductivity and suitable energy band alignment.[41, 51, 52] You et al.[41] fabricated ST PSCs by laminating stacked multilayer graphene as the transparent top electrode. They prepared highly conductive graphene electrode with a poly(3,4-ethylenedioxythiophene): poly(styrenesulfonate) (PEDOT:PSS) film. The fabricated devices showed maximum PCEs of 12.02% and 11.65%

when illuminated from the fluorine-doped tin oxide (FTO) and graphene sides, respectively. ST PSCs with a transmittance of approximately 50% at 700 nm showed an average PCE of 5.98% and 5.70%, from the FTO and graphene sides, respectively. The application of graphene in PSCs not only reduces the manufacturing cost, but also significantly improves the cell stability owing to its hydrophobic nature.[53] Very recently, Zhang et al.[54] reported an innovative strategy to construct PSCs using graphene-coated FTO electrodes as cathodes, where the light transmittance of the spray-coated graphene film was around 30% at a wavelength of 550 nm (Figure 3d). A modular PSC, fabricated using this graphene electrode, exhibited a high PCE of 18.65% when illuminated from the anode side, and 6.33% when illuminated from the graphene cathode side (Figure 3d). Moreover, the device was stable for at least 6000 h in ambient air storage. This suggests that high-efficiency ST PSCs with excellent AVT can be fabricated using the method reported in this work. Future studies should focus on increasing the transparency of graphene films while maintaining high conductivity, which will allow for the fabrication of high-efficiency ST PSCs without metal electrodes.

In addition to CNTs and graphene, two-dimensional (2D) MXene ($Ti_3C_2T_x$) was recently found to be a promising candidate for hole-transporting-material (HTM)-free and noble-metal-free PSCs.[55] Other studies have also demonstrated that 2D MXene nanosheets show excellent electrical conductivity and high optical transparency.[56, 57] Therefore, it is reasonable to expect that highly efficient and stable ST PSCs can be created by employing a thin 2D MXene film as the top electrode. The use of functionalized MXene nanosheets for PSCs is also an important research direction.

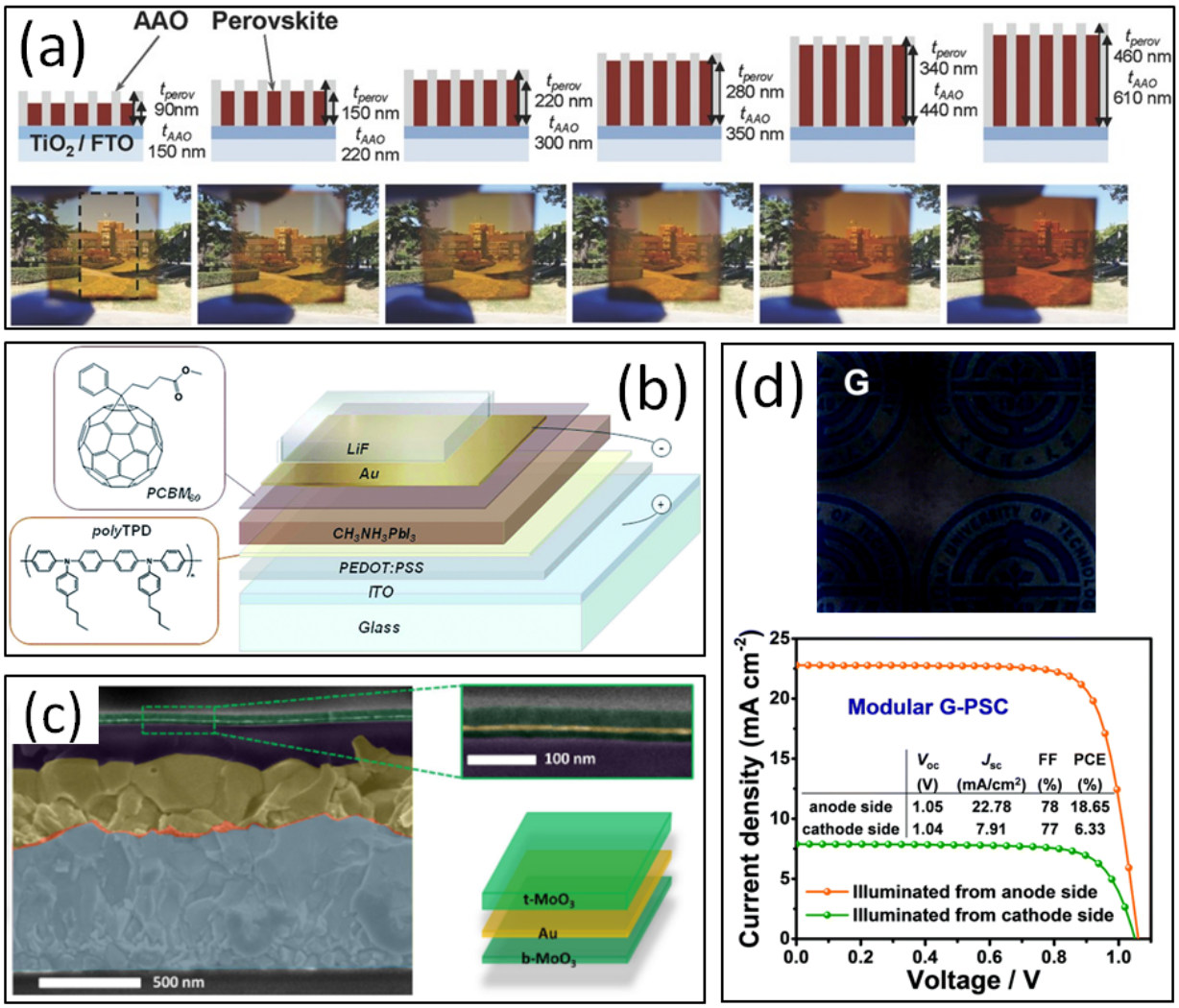

Figure 3. (a) Schematic illustration of spin-infiltrated perovskite layers, in anodic aluminum oxide (AAO) templates, with different thicknesses and the corresponding perovskite films. Reproduced with permission.[49] Copyright 2016, WILEY-VCH. (b) Schematic showing an inverted PSC fabricated with a LiF capping layer. Reproduced with permission.[39] Copyright 2014, The Royal Society of Chemistry. (c) Cross-sectional SEM image of a full device fabricated with a dielectric–metal–dielectric (DMD) (MoO_3–Au–MoO_3) multilayered top electrode. Reproduced with permission.[50] Copyright 2015, Elsevier. (d) Spray-coated graphene film on FTO substrate. J–V characteristics of modular PSC fabricated using spray-coated graphene film. Reproduced with permission.[54] Copyright 2019, The Royal Society of Chemistry.

Although great developments in the fabrication of ST PSCs have been achieved over the past few years, practical integration of these PV cells into building applications remains a

challenge. Integrating ST PSCs into buildings is advantageous only if the energy benefits of BIPVs outweigh the costs. Cannavale et al.[58] estimated the annual energy production and visual comfort benefits of ST perovskite PV windows with a PCE of 6.64% and an AVT of 42.4%. The effects of different climate conditions and two window-to-wall ratios (19% and 32%) for office buildings were taken into consideration. The authors found that the annual energy production of such PV windows could be higher than the amount of electric energy used for artificial lighting in most cases.

In general, an AVT of 25% is considered a benchmark for solar windows. However, it will be difficult to produce a large amount of current if a quarter of the light is transmitted through the window. It should be noted that PV efficiency depends on two important factors: current and voltage. Therefore, one way to achieve high-efficiency ST PSCs is to improve the cell voltage to compensate for the lower cell current. In this regard, compositional engineering of perovskite materials is an effective way of adjusting the band energy of perovskite.[59]

Furthermore, toxicity and stability are the major hurdles to successful integration of ST PSCs into buildings. A common concern is the inclusion of lead (Pb) as a component of perovskite materials. Substituting Pb with other non-toxic materials, such as tin (Sn), antimony (Sb), and bismuth (Bi), has shown promise, but reduces efficiency. Therefore, it is important to explore other ways to enhance the PV performance of lead-free PSCs. More importantly, encapsulation techniques should be pursued, to improve the long-term stability and address the potential issues associated with the toxicity of lead-based ST PSCs.

It is worth noting that excellent progress has been made in enhancing the PV efficiencies of ST PSCs. These highly efficient ST PSCs, however, have so far used only small, prototype-scale cells. For the commercialization of ST PSCs as solar windows, highly efficient transparent cells with typical window dimensions will be required.

3. Colorful PSCs

Colorful PSCs are desirable for BIPVs and other applications where aesthetics are important. The color of a perovskite film is strongly dependent on its light absorption spectrum and bandgap.[60] The bandgap of a perovskite can be tuned by adjusting the elemental components.[20, 61] A digital photo of the most commonly used lead-halogen perovskites is presented in Figure 4a. Noh et al.[60] were the first to report on the chemical management of $MAPb(I_{1-x}Br_x)_3$ perovskites for colorful PSCs. The authors successfully tuned the onset absorption band of the perovskites from 786 nm (1.58 eV) to 544 nm (2.28 eV) by tuning the Br content (Figure 4b). By optimizing the amount of Br in the perovskite, the best-performing colorful PSC delivered a PCE of 12.3%, which was an impressive performance for a device in 2013. Furthermore, Zhang et al.[62] used a porous photonic crystal scaffold within the light-harvesting layer of an opaque PSC. The fabricated PSCs showed tunable colors across the visible spectrum and achieved an efficiency of up to 8.8% with a blue hue. A simple doctor-blade coating method was used by Huang's group to prepare vividly colored perovskite films (Figure 4c).[63] Spontaneous formation of the photonic structures in these perovskite films was readily scalable for the fabrication of colorful PSCs with large areas (Figure 4d).

In addition to the chemical management of perovskite precursors, optical configurations have been designed to adjust the color of PSCs without changing the inherent properties of perovskite films. This strategy was developed by Lee et al.[64] who used a dielectric film to separate two optically thin metallic layers, forming a metal/dielectric/metal (MDM) microcavity electrode. Promisingly, by simply changing the thickness of the dielectric layer, they could tune the resonance transmission of a specific wavelength of visible light (e.g., transmitting red, green, and blue colors). However, the highest efficiency of the ST PSC fabricated with this configuration (with an $Ag/WO_3/Ag$ electrode) was only 3.86%, with a red device. Similarly, Lu et al.[65] designed Ag/ITO/Ag microcavity electrodes for the fabrication of colorful ST PSCs. Upon varying the thickness of the top ITO layer, the device color could

be tuned from reddish-orange to blue. The highest PCE (7.6%) was obtained using a bluish-green ST PSC.

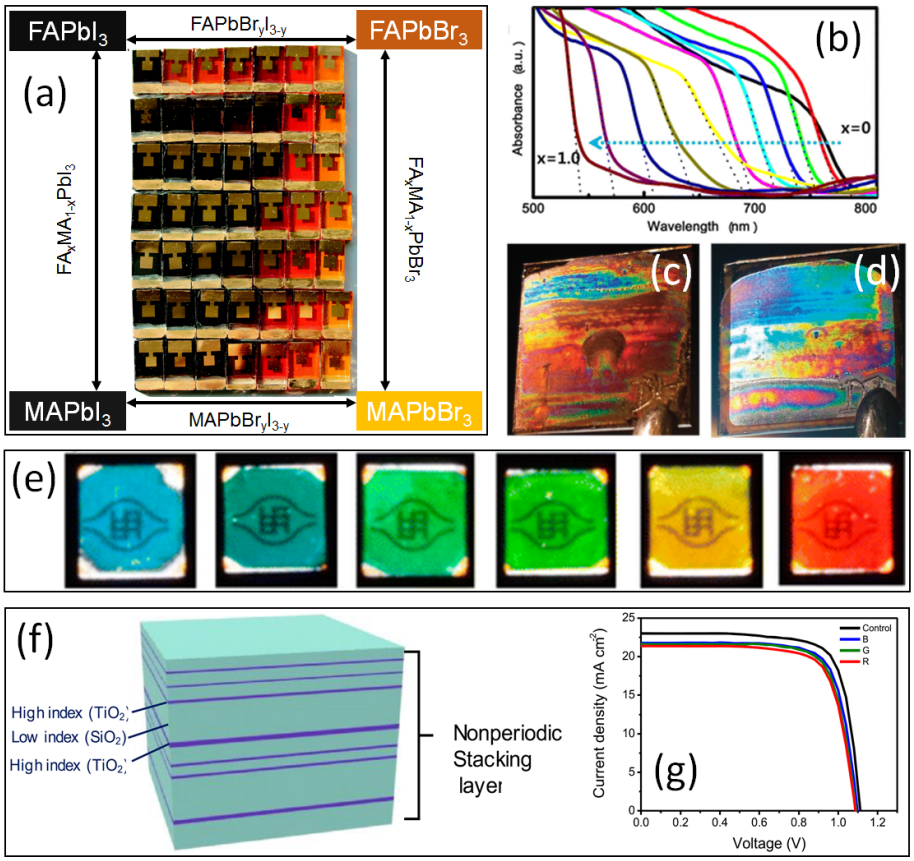

Figure 4. (a) Photograph of the commonly used perovskite absorber-based PSCs with Spiro-OMeTAD as an HTM and Au electrode. Reproduced with permission.[61] Copyright 2016, The Royal Society of Chemistry. (b) UV-vis absorption spectra of FTO/bl-TiO_2/mp-TiO_2/$MAPb(I_{1-x}Br_x)_3$/Au cells measured using an integral sphere. Reproduced with permission.[60] Copyright 2013, American Chemical Society. (c) Photograph of the as-prepared colorful perovskite film and (d) the corresponding PSC with an aluminum electrode on top. Reproduced with permission.[63] Copyright 2015, The Royal Society of Chemistry. (e) Photograph of microcavity-based colorful ST PSCs. Reproduced with permission.[65] Copyright 2016, American Chemical Society. (f) Schematic diagram of the structure formed through nonperiodic stacking of high-refractive-index (TiO_2) and low-refractive-index (SiO_2) layers. (g) J–V curves of the PSCs with red, green, and blue colors obtained with the structure described in (f). Reproduced with permission.[21] Copyright 2016, American Chemical Society.

Quiroz et al.[66] combined ST PSCs with dielectric mirrors, which are made of alternating layers with a high refractive index and a low refractive index. By using this strategy, any desired device color could be achieved while the dielectric mirrors were also able to enhance the light harvesting efficiencies of the devices. A PCE of 4.2% was obtained for the colored ST PSC with 31.4% transmittance. Furthermore, colorful ST PSCs were prepared using simple spin-coating of different color pigments onto typical PSC devices.[34] The authors first fabricated a $CH_3NH_3PbI_{3-x}Cl_x$ perovskite-based ST PSC with a PCE of 5.36% at an AVT value of 34%. Subsequently, pigments of different colors (green, yellow, and red) were diluted with propylene glycol 1-monomethyl ether 2-acetate, and the solution was gently spin-coated onto the Au surface.

In the same year (2016), a group of researchers led by Zhou used a transparent conducting polymer (PEDOT:PSS) as a top electrode, as well as a spectrally selective antireflection coating, to fabricate colorful PSCs.[67] The color of the PSCs could be tuned across the visible spectrum by engineering optical interference effects among the transparent PEDOT:PSS electrode, the hole-transporting layer, and the perovskite layer. When illuminated from the FTO side, the colorful PSCs, with PEDOT:PSS thicknesses of 75, 95, 105, and 160 nm, displayed PCEs in the range of 15–16%, while their AVT values were approximately 10%.[67] This simple approach provides an efficient method for obtaining high-efficiency colorful PSCs.

Very recently, highly efficient colorful (red, green, blue) PSCs were fabricated by Yoo et al.[21] who prepared narrow-band-width reflective filters (NBRFs) by stacking many alternating layers of high-index TiO_2 and low-index SiO_2 in a nonperiodic manner. By exploiting the optical properties of these multilayered NBRFs, PSCs with red, green, and blue colors exhibited PCEs of 18%, 18.6%, and 18.9%, respectively, while the black control PSC had an efficiency of 20.1%. Moreover, these colorful PSCs showed excellent photostability when compared to the control device, due to the TiO_2 layers blocking UV light. This study

reported PSCs with a combination of aesthetic color value, high PCE, and enhanced photostability, all of which suggest their great potential for use in power generation on building exteriors. Based on the high efficiencies obtained by Yoo et al.[21] colorful PSCs with PCEs of over 20% can be expected in the near future. Future studies should also focus on improving the AVT of such high-efficiency, colorful PSCs. Moreover, the use of transparent conducting surface electrodes such as PEDOT:PSS, graphene, and CNTs in this class of solar cell is expected to bring significant development to colored ST PSCs.

4. Perovskite Photovoltachromic Windows

Residential and commercial buildings account for a considerable fraction of the energy used for heating, ventilation, and air conditioning (HVAC), but nearly 50% of that energy is generally wasted due to unwanted heat exchange through conventional windows.[68, 69] Smart windows are regarded as an efficient and promising green technology because they not only reduce cooling/heating costs and ventilation loads, but also improve privacy protections.[70, 71] Smart windows are made from electrochromic, photochromic, and thermochromic glasses that can adjust their optical transmission properties in response to an external stimuli (e.g. voltage, light, or heat).[72] As a type of smart PV window (SPW), PVCCs have gained much attention owing to their ability to integrate power (electricity) generation, energy saving, and privacy protection into a single device.[73, 74]

PVCCs combine PV devices and electrochromic functions to control reversible redox switching between the bleached and colored states.[75] In PVCCs, PV cells provide an electrical supply to drive the coloration. An ideal electrochromic material should provide high optical contrast, fast switching kinetics, and high coloration efficiency, while the PV device should exhibit a high PCE.

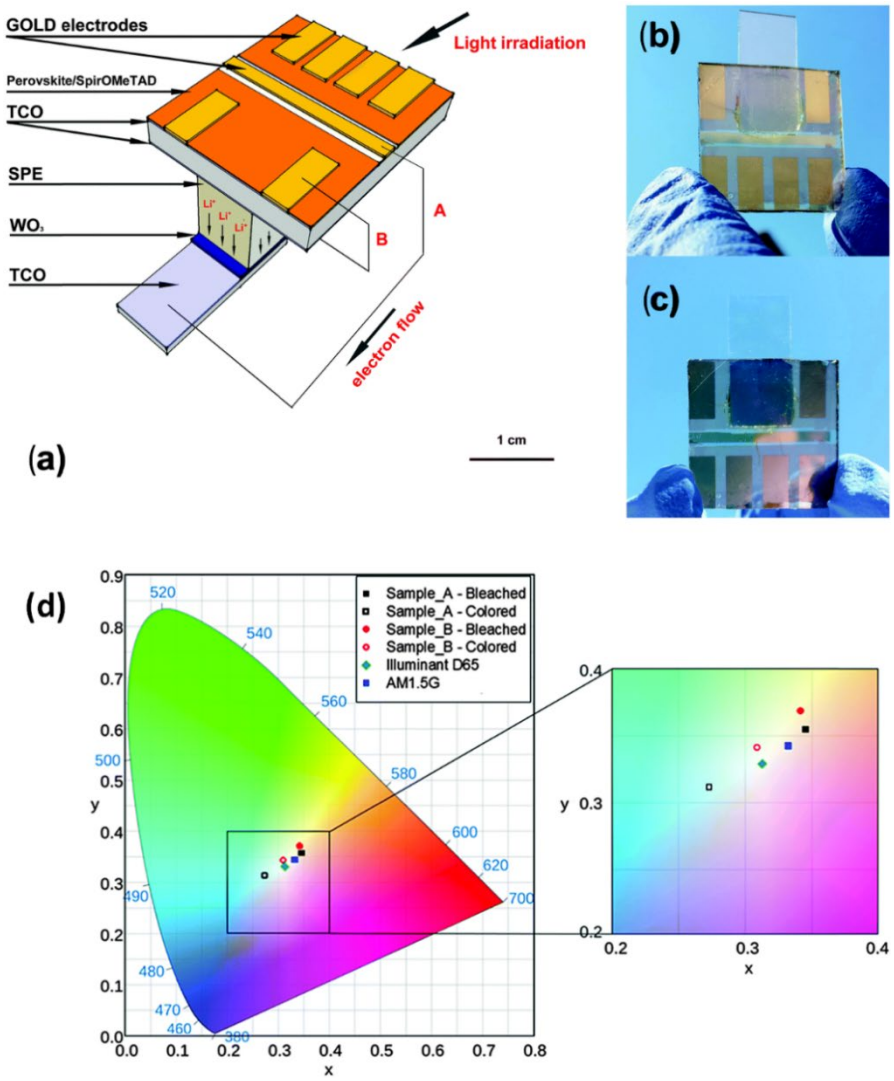

Figure 5. (a) Schematic illustration of the PSC-based PVCC device. (b) Pictures of the first PVCC device under (b) bleached and (c) colored conditions. (d) Color coordinates of the PVCCs under AM1.5 illumination, plotted on the CIE xy 1931 chromaticity diagram, and the enlarged central region. For comparison, color coordinates of the D65 standard daylight and AM1.5 illumination are also displayed. Sample A: the PVCC device with high AVT; Sample B: the device with low AVT. Reproduced with permission.[22] Copyright 2015, The Royal Society of Chemistry.

As the next generation of PVs, PSCs have recently been demonstrated as promising devices for PVCCs, due to their high efficiency and excellent transparency. Cannavale et al.[22] conducted the first study employing a PSC as the power supply of a PVCC whereby a PV device and electrochromic layers were deposited on two separated glass sheets (Figure 5a). Without any additional external bias, the device changed color from neutral ST (15.9% AVT)

to a dark blue tint (5.5% AVT) when illuminated (Figure 5b and 5c), and exhibited a maximum PCE of 5.5% in the colored state. Figure 5d depicts the color coordinates of the transmission through the whole active region of two devices in both bleached and colored states, in comparison to the reference daylight illuminant D65 and the AM1.5 spectrum. The PVCCs fabricated by Cannavale et al.[22] were found to have good color-neutrality in the bleached state, which was close to the AM1.5 spectrum, making PSC-based PVCCs promising candidates for building integration. This pioneering work has led to the recent focusing of effort on the development of perovskite-based PVCCs.

In conventional PVCCs, the electrical power produced from the PV cells is only used to alter the optical transmittance of the chromogenic electrodes.[22, 75, 76] Therefore, the devices are not able to store harvested solar energy. In this regard, integrating PV cells with both energy storage devices and electrochromic layers would result in sustainable green technology that can generate and store power, while automatically tuning the optical transmittance. In 2016, Zhou et al.[26] integrated an ST PSC and electrochromic WO_3 supercapacitor into a photovoltachromic supercapacitor (PVCS). The fabricated PVCS showed excellent integration of an energy production and storage device, automatic color tunability, and enhanced photostability of PSCs. The top Au electrode of a typical PSC (with 16.4% efficiency) was replaced with a stacked transparent structure of spiro-OMeTAD/Au/MoO_3 (15 nm/12 nm/20 nm). This device exhibited an impressive AVT of 70.6% and decent PCEs of 12.54% and 9.35%, when illuminated from the FTO side and MoO_3/Au/MoO_3 side, respectively. The measured energy density, power density and areal capacitance of the co-anode and co-cathode PVCS were 13.4 and 24.5 mWh/m^2, 187.6 and 377.0 mW/m^2, and 286.8 and 430.7 F/m^2, respectively. Importantly, the electrochromic shelter of the PSC could change color from ST to dark-blue, with AVT reduction from 85% (76.2%) to 35.1% (23.0%) for the co-anode (co-cathode) PVCS.[26]

Another example of integrating PSCs with energy storage devices for smart windows was reported by Xia et al. who constructed a novel type of electrochromic battery powered by PSCs.[25] In this work, an HTM-free PSC, with a porous carbon electrode and a highly stable PCE of 11.9%, was fabricated using a low-cost and simple process. The electrochromic batteries were made of reduced graphene (rGO) coupled with a bilayer NiO nanoflake array cathode and a WO_3 nanowire array anode. The fabricated device showed relatively fast (2.5–2.6 s) and wide optical modulation of up to 62% in the NIR range. Moreover, the electrochromic battery constructed in this work exhibited a capacity of 75 mA h g^{-1} at 1 A g^{-1} with good cycling life. This class of PV-integrated electrochromic energy storage system is very promising in that it can exhibit a wide range of functionalities, such as solar energy harvesting, electrochemical energy storage, and reutilization, in addition to the optical transmission. Since the optical performance achieved by the electrochromic layer in this work is very promising, future studies should focus on increasing the battery performance by employing high-performance cathode materials.

Over the past half-decade, we have witnessed a significant step forward in PSC-integrated SPWs. Despite the remarkable acceleration in this cutting-edge research field, the fabricated PVCCs suffer from at least one of the following limitations: low PCE, poor device stability, long response time, and poor responsive behavior. Some of these limitations have been addressed, but at a cost to the others.[22, 26] Recently, Xia and co-workers made an important contribution to the field of SPWs by integrating ST PSCs with multi-responsive liquid crystal/polymer composite (LCPC) films.[23] Stimuli-responsive LCPC films were used as an inside layer on the device to modulate the optical transparency of the SPWs. The as-prepared LCPC films were highly responsive to temperatures (Figure 6a) and external electric fields (Figure 6b), with outstanding switchable stability. As an outside layer, ST PSCs with a layered structure of FTO/Au-SnO_2/$(FAPbI_3)_x(MAPbBr_3)_{1-x}$/Spiro-OMeTAD/Au were fabricated and used. This PV device, with an AVT of slightly higher than 10%, exhibited a

PCE of 16.67% which is remarkable efficiency for ST PSCs. When these two systems are combined (ST PSC and LCPC), the SPW showed multiple distinct working modes benefiting from the multi-responsive behavior of the LCPC layer. In particular, at room temperature, the integrated device exhibited a similar transparency state as the ST PSCs, due to high transparency of the LCPCs at low temperature. Upon heating to only 40 °C, the device turned opaque owing to the strong light-scattering state of the LCPCs. By applying an external electric field, the ST PSC/LCPC device can be returned to the ST state, even at 40 °C. All of these attractive features of this integrated device are illustrated in Figure 6c. It is very promising that this device is highly responsive to different conditions, including low temperatures (e.g. 40 °C), which can be achieved on a hot summer day. It can be expected that when temperatures reach ~40 °C, this type of SPW will be able to generate high power output and become non-transparent. Thus, the opaque color of the windows can be utilized to both save energy and protect privacy. Moreover, if preferred, the transparency of the window can be manipulated by applying an external electric field. Therefore, these findings reported in this exciting work by Xia et al.[23] show great promise for the future development of perovskite-based SPWs. However, it should be noted that in their work, the electric field (up to 55 V) used to modulate the optical transmittance was externally supplied. As such, developing self-powered SPWs with high PV efficiency and excellent degree of color tunability is of great value. In addition, research on developing lead-free PSC-based PVCCs and SPWs would be of great interest.

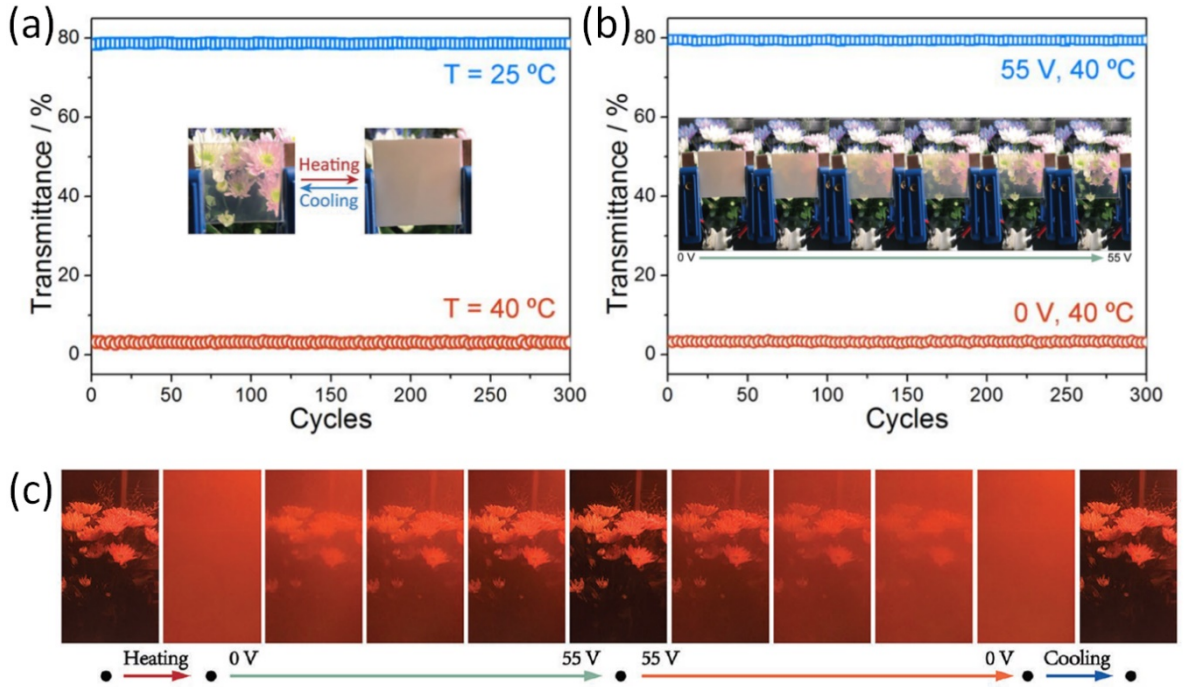

Figure 6. Transmittances of the LCPC films at 550 nm under repeated (a) heating/cooling (inset shows the photographs of LCPC film at these two phases), and (b) electric field on/off process (inset shows the photographs of LCPC film under various voltages between 0 and 55 V). (c) Photographs of ST PSC-integrated LCPC film with controllable transparency stimulated by temperature and electrical field. Reproduced with permission.[23] Copyright 2019, WILEY-VCH.

5. Thermochromic Perovskites for SPWs

Smart solar windows have been around for years. In 2015, PSCs were integrated with electrochromic windows (see section 4), forming a new kind of SPW.[22] Perovskites exhibit a comprehensive range of fascinating features including tunable color, a high absorption coefficient and long charge diffusion length.[3-5] Indeed, in early-2017, Bakr's group reported for the first time that perovskites show outstanding thermochromic properties.[29] The unusual crystallization behavior of halide perovskites plays an important role in their thermo-responsive behavior. The solubility of perovskites decreases as the temperature increases, resulting in single-crystal cell nucleation and growth of single perovskite crystals.[14] As the

temperature further increases, the band gap shift, and change in optical properties, can be observed.

Bakr et al.[29] prepared an $MAPb(I_{1-x}Br_x)_3$ perovskite ink with a dense yellowish color at room temperature (25 °C). The perovskite ink was then heated to different temperatures to observe its thermochromic variations. The ink color changed to orange upon heating to 60 °C and to bright red at 90 °C. Finally, the color of the ink turned to black when the temperature reached 120 °C. The color changes and the corresponding light absorption spectra of the ink at different temperatures are illustrated in Figure 7a-c. In Figure 7c, the absorption red shift induced by the temperature increase suggests that perovskite ink is strongly thermochromic. The authors also found that this excellent temperature-induced chromatic variation is highly reversible in the presence of solvents. Therefore, a prototype thermochromic window was fabricated by sealing the perovskite ink inside a glass cuvette (Figure 7d). With a conversion time of just a few seconds, the color of the prototype window could be changed by heating it to 60 °C. As shown in Figure 7e, the band edge variation of the prototype under consecutive cycles suggests that this perovskite-ink window can be reproduced with high fidelity. This pioneering work by Bakr's group opened up a new avenue for smart windows that used perovskite inks as both the stimuli-responsive thermochromic component and light-harvesting material. Notably, the halogens are the main components that determine the crystallization temperature of perovskites. Therefore, introducing new halide components would be an effective strategy for controlling the thermochromic properties of halide perovskites.

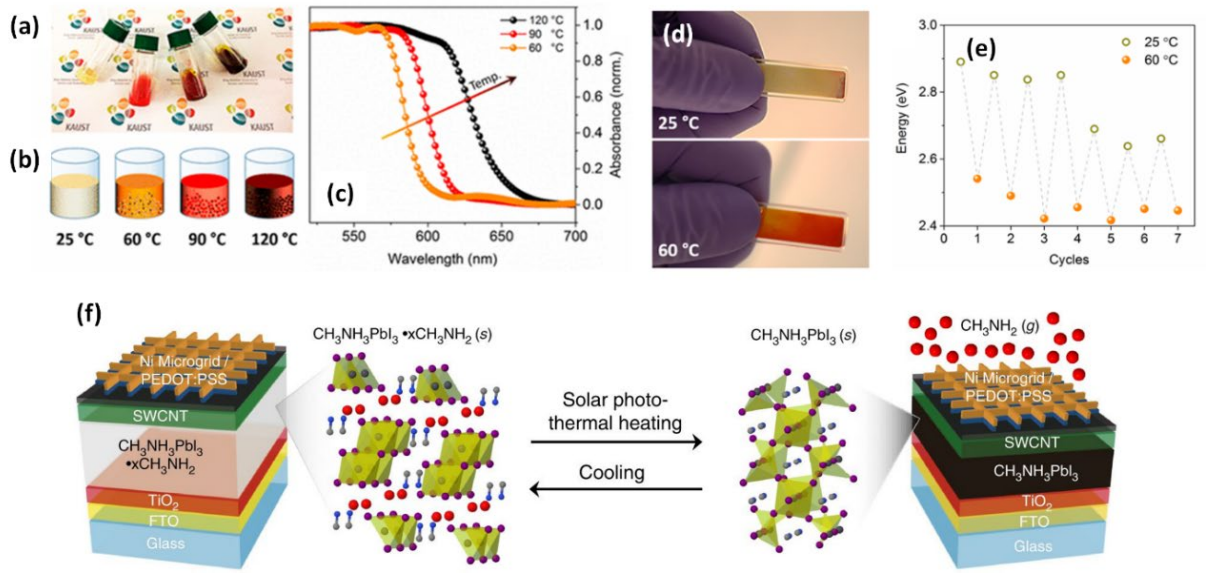

Figure 7. (a) Photograph and (b) schematic illustration of thermochromic perovskite inks at 25, 60, 90 and 120 °C. (c) Absorption spectra of precipitated solids collected from the perovskite inks. (d) Photograph of the prototype thermochromic perovskite-ink window at 25 °C (top) and 60 °C (bottom) and (e) the corresponding band edge variation. (a-e) Reproduced with permission.[29] Copyright 2017, American Chemical Society. (f) Schematic of SPW device architecture and its switching process. Reproduced under the terms of the Creative Commons CC-BY license.[28] Copyright 2017, Springer Nature.

Indeed, the first advance in combining thermochromic perovskite and light-harvesting perovskite into a single SPW was reported by Wheeler et al.[28], who designed a lead-based perovskite solar window that can switch from transparent to opaque at 60 °C. They demonstrated the formation of a methylammonium lead iodide-methylamine complex ($CH_3NH_3PbI_3$•xCH_3NH_2) for a switchable PV window that adapts its absorption properties to solar conditions without pairing separate electrochromic and PV cells. In this switchable SPW, perovskite forms a complex with the xCH_3NH_2 at cooler temperatures. Upon heating (solar photo-thermal heating), the perovskite darkens and absorbs sunlight as the xCH_3NH_2 vaporizes away from the $CH_3NH_3PbI_3$. When the heat dissipates or when the sun goes down (cooled down), the xCH_3NH_2 returns to its complexed bleached state (see Figure 7f). The warmed devices achieved solar energy conversion efficiencies of up to 11.3% in the colored

state, and high visible light transmittance of 68% in the bleached state. This work potentially addresses the fundamental limitation associated with the tradeoff between PCE and transparency observed in conventional ST solar windows. Due to its high efficiency and excellent optical transmission, this halide-perovskite-based SPW technology may provide great opportunities for many advanced applications including building integrations.

Despite many promises, the SPW designed by Wheeler et al. suffers from a drop in PV efficiency after switching only a few times between the bleached and colored states. In early-2018, Yang's group created an all-inorganic perovskite-based thermochromic SPW that turns opaque and generates power when heated,[30] but without the use of additional components such as $x CH_3NH_2$. This smart solar window was realized based on the structural phase transitions of the inorganic halide perovskite, cesium lead iodide/bromide ($CsPbI_{3-x}Br_x$). Reversible transitions between a transparent non-perovskite phase with an AVT of 81.7% and a deeply colored perovskite state with 35.4% AVT were controlled by thermal heating (105 °C) and moisture exposure. The window exhibited excellent stability under consecutive phase transition cycles, without color fading or performance degradation. The fabricated SPW achieved a peak PCE of more than 7% using colored perovskite in the low-transparency state, whereas the transparent solar cells with a non-perovskite phase had efficiencies of less than 0.2%. In spite of their fascinating features, thermochromic perovskite-based SPWs still need significant development, and efforts should be made with a great sense of urgency. For instance, the SPWs designed by Yang's group still require high temperatures (> 100 °C) to switch from the transparent to opaque state. As such, exploring thermochromic perovskites that switch colors at low temperature (<50 °C) would be valuable. This will enable SPWs to operate themselves by switching to an opaque state while producing electrical power during a hot summer. The slow phase transition of the perovskites, especially in moisture, remains an issue, and moreover, the maximum efficiency of the SPW fabricated by Yang's group was only ~7%. Clearly, other strategies and designs should be pursued to enhance the PV

efficiency of SPWs. Considering the toxicity of lead-based perovskites, designing lead-free perovskites that can exhibit high PV efficiency, excellent stability and thermochromic behavior is of great importance. Recently, Ning et al.[77] developed thermochromic lead-free perovskite ($Cs_2AgBiBr_6$) crystals which exhibit excellent reversible thermo-responsive properties (see Figure 8). However, the PV properties and performance of this lead-free perovskite were not explored. Furthermore, the current thermochromic perovskite windows fail to modulate light transmittances in the NIR range. In addition to ITO electrodes, other TCEs such as those based on graphene,[78] metal nanowires,[79] and CNTs[80] should be employed as efficient top electrodes in perovskite-based SPWs. Nevertheless, future research is expected to focus on SPWs, in particularly perovskite-based ones.

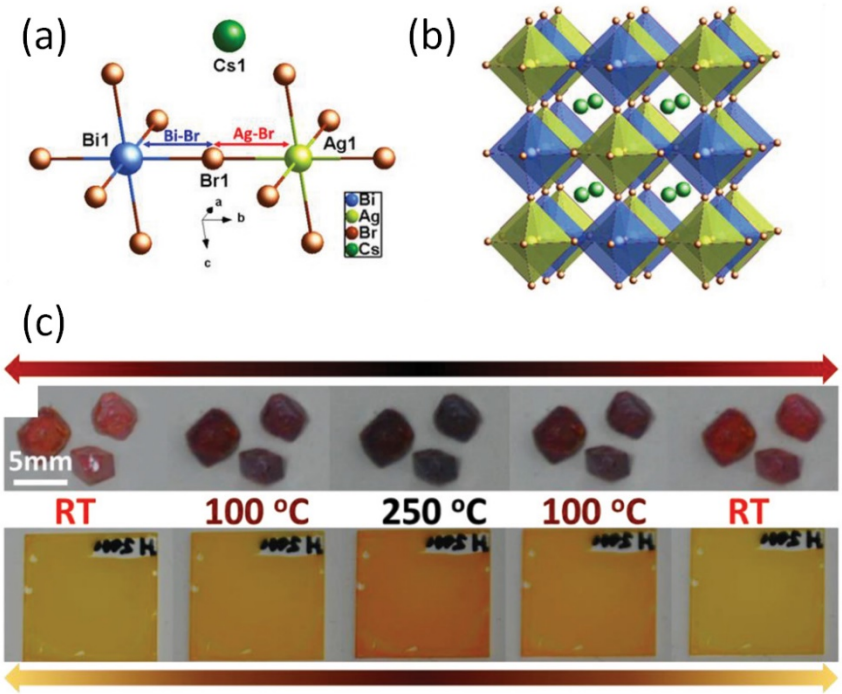

Figure 8. (a) Molecular structure and (b) packing structure of Pb-free $Cs_2AgBiBr_6$ single-crystal perovskite. (c) Optical images of single $Cs_2AgBiBr_6$ crystals and thin films at different temperatures during one heating–cooling cycle. Reproduced with permission.[77] Copyright 2019, WILEY–VCH.

Table 1. Summary of advantages, challenges, and possible solutions of perovskite-based BIPVs. Detailed roadmaps for their future development of perovskite-based BIPVs are provided in the Conclusion section.

Category	**Advantages**	**Key references**	**Challenges**	**Possible solutions**
ST PSCs for facades, windows, and glass roofs	- Reducing incident heat gain - Generating power (electricity) - Various configurations	[39], [40], [41], [42], [43], [47]	- Low visible transparency - Limited cell efficiency - Poor stability	- Using emerging TCEs such as graphene and CNTs as the top electrode - Designing new perovskite structures - Device encapsulation
Colorful PSCs for walls, windows, and roofs	- Various colors - Generating power (electricity) - High efficiency	[21], [34], [60], [62], [66], [67]	- Poor PV performances for ST devices - Stability issues	- Exploring new designs for colorful ST PSC devices - Reporting stability test of the devices
Dual functional PVCCs for windows, facades, and parking roofs	- Energy saving/privacy protection - Smart windows - Generating power (electricity) - Possible integration of energy storage devices	[22], [23], [25], [26]	- Long stimuli-response time - Limited cell efficiency - Stability issues	- Utilizing new electrochromic materials - Developing highly efficient ST PSCs - Testing long-term stability of the PVCCs - Using carbon top electrodes and device encapsulation
Thermo-chromic solar cells for windows, facades, and parking roofs	- Energy saving - Smart windows - Simple design - Generating power (electricity)	[28], [29], [30]	- Poor cyclability and stability - Slow stimuli-response - High operation temperature - Low PV efficiency	- Exploring components that are stable during cycling - Designing new perovskite structures with high stimuli-response - Developing perovskites that can be reversed at low temperature

6. Conclusion

Perovskites are promising candidates for BIPVs owing to their tunable bandgap, high absorption coefficient, high PV efficiency, and good optical transparency. In particular, perovskites play a significant role in the four classes of BIPVs, namely ST PSCs, colorful PSCs, PVCCs, and thermochromic perovskite SPWs. In this Progress Report, we have summarized the recent advancements and notable achievements in the field of perovskite-based BIPVs. It is clear that this cutting-edge research field is still in its initial stage, and further developments are required. Table 1 summarizes the advantages, challenges, and future directions of perovskite-based BIPVs. Therefore, we believe that the following points will be of great importance and should be considered carefully in future studies on perovskite-based BIPVs.

(i) Island-structured perovskite films with incomplete coverage, obtained using a de-wetting method, are an effective strategy for preparing neutral ST PSCs. However, in order to prevent direct contact between the electron and hole transporting layers, the use of other layers such as the shunt-blocking layer and passivation layer is necessary.[45, 46] Researchers should explore the use of other effective layers that not only block shunting between the charge transporting layers but also possess extra functionalities, such as light harvesting. The structural management of perovskite layers is a promising method of fabricating efficient ST PSCs. More attention should be paid to the development of novel structural designs for perovskite growth. Considering the simplicity, previously established techniques such as etching, texturing, and other effective deposition strategies that can be used to precisely control the growth of the perovskite should be explored.

In general, ST PSCs are fabricated using thin metal (Au or Ag) films with some additions of top electrodes. Emerging TCEs such as graphene, CNTs, and Ag nanowires are promising candidates for a wide range of PV applications owing to their high electrical conductivity and excellent optical properties. For instance, graphene shows much higher transparency in the

near-infrared region as compared to ITO and FTO.[81] The conductivity of graphene electrodes can be improved using doping techniques. The use of graphene as a top electrode in ST PSCs has clear advantages in terms of the manufacturing cost, optical transparency, and long-term stability of the devices. As such, future studies should aim to develop high-performance BIPVs using emerging TCEs.

(ii) Colorful PSCs are suitable for use in power-generating building exteriors, such as walls and parking roofs, owing to their promising device efficiency and wide selection of colors. By using simple spin-coated pigments of the desired colors, highly efficient PSCs can be prepared in a range of colors. Furthermore, recent studies have shown that various colored PSCs, with PCEs of nearly 20%, can be fabricated using creative designs such as narrow-bandwidth reflective filters. Although excellent progress has been made, the stability of these solar cells remains a significant limitation to future commercialization. Furthermore, while optically transparent colorful PSCs are of particular interest for building integration, they suffer from low device efficiencies due to their limited light absorption. Optical configuration using a microcavity electrode, such as MDM, is a promising strategy for the fabrication of colorful ST PSCs, but their current efficiencies are still less than 10%. Therefore, there is a need to develop novel cell designs that can be used to fabricate colorful PSCs with remarkable efficiencies and high AVTs.

(iii) Despite the potential promises of PVCCs, reports on PSCs integrated with PVCCs are lacking. Although a large variety of electrochromic materials are available, only a few of them, such as LCPC and WO_3, have been used for PSC-based PVCCs. Exploring the suitability of other promising electrochromic materials, including MoO_3, TiO_2, NbO_x, MoS_2, and MXene, for PVCCs would be of great value. Furthermore, researchers should also focus on developing single PVCC devices by attaching PSCs to electrochromic windows. In this class of PVCC, the optical transparency of the PSC plays a vital role in window performance.

As such, high-efficiency ST PSCs will be required. Future work should also aim to develop self-powered SPWs with high PV efficiency, instead of applying an external electric field. Integrating PSCs with energy storage devices (batteries) and electrochromic windows is an interesting strategy for creating devices with multiple functions, including power generation, storage, and optical modulations. However, this class of PV-integrated electrochromic battery is currently suffering from low performance. Although some studies on PSC-integrated PVCCs tested the cycling stability of the devices, the long-term stabilities of the fabricated devices in both ambient environments and operating conditions should be investigated in the future. Carbon-based top electrodes are promising candidates for fabricating highly stable PSCs.

(iv) The use of perovskites as both stimuli-responsive (thermochromic) components and light-harvesting materials in SPWs is a very recent scientific breakthrough. Although several excellent advancements have been made in this cutting-edge research area, thermochromic perovskite smart windows still suffer from many issues. One of these issues is the rapid decline in efficiency during cycling, mainly due to the unstable perovskite component that fails to fully switch between non-crystal and crystal structures. Time delays in switching between transparent and opaque states of thermochromic PSCs is another considerable drawback. Another significant issue is that currently, thermochromic perovskite smart windows require high operational temperatures (more than 100 °C), which are impractical. Hence, there is a pressing need to design novel perovskite structures that are stable under various experimental conditions and can be operated at low temperatures while exhibiting fast stimuli-responsive behavior. The combination of perovskites with other efficient thermochromic materials in a single SPW may be an efficient strategy for obtaining windows that have both high PV efficiency and excellent thermo-responsiveness.

Current perovskite-based BIPVs mainly employ lead-based components owing to their ability to deliver high PV performances. However, considering their toxicity, it is important to

develop lead-free perovskites that can exhibit high PV performance, excellent stability, and low costs. As highlighted in Table 1, the long-term stability is one of the main limitations for building integration of all categories of perovskite-based devices. Therefore, it is necessary to make perovskite devices that are stable under various conditions, particularly in high humidity environments with extreme temperature variations. One promising strategy to increase the lifetime of perovskite-based devices is through effective encapsulation techniques that can successfully protect solar cells from moisture, UV-light degradation, and oxidation. Carbon-based top electrode materials, such as porous carbon, graphene, CNTs, and MXene and their functionalized derivatives, have the potential to not only improve device stability under ambient conditions, but can also enhance PV performance. Moreover, developing these perovskite-based BIPVs with good flexibility and substrate conformity would create more avenues for building integrations. In conclusion, we anticipate that this progress report will provide important insights into the future development of perovskite-based BIPVs.

Acknowledgements

The authors acknowledge the support from the Australian Research Council (LP160101521). Munkhbayar Batmunkh acknowledges the support of Griffith University 2020 New Researcher Grant (GU NRG).

Received: ((will be filled in by the editorial staff))
Revised: ((will be filled in by the editorial staff))
Published online: ((will be filled in by the editorial staff))

References

[1] M. A. Green, A. Ho-Baillie, H. J. Snaith *Nature Photon.* **2014**, 8, 506-514.
[2] A. Kojima, K. Teshima, Y. Shirai, T. Miyasaka *J. Am. Chem. Soc.* **2009**, 131, 6050-6051.
[3] N.-G. Park, M. Grätzel, T. Miyasaka, K. Zhu, K. Emery *Nat Energy.* **2016**, 1, 16152.
[4] C. Zuo, H. J. Bolink, H. Han, J. Huang, D. Cahen, L. Ding *Adv. Sci.* **2016**, 3, 1500324.
[5] A. S. R. Bati, M. Batmunkh, J. G. Shapter *Adv. Energy Mater.* **2020**, 10, 1902253.
[6] H. J. Snaith *J. Phys. Chem. Lett.* **2013**, 4, 3623-3630.
[7] J. Burschka, N. Pellet, S.-J. Moon, R. Humphry-Baker, P. Gao, M. K. Nazeeruddin, M. Grätzel *Nature*. **2013**, 499, 316-319.
[8] N.-G. Park *J. Phys. Chem. Lett.* **2013**, 4, 2423-2429.

[9] H.-S. Kim, C.-R. Lee, J.-H. Im, K.-B. Lee, T. Moehl, A. Marchioro, S.-J. Moon, R. Humphry-Baker, J.-H. Yum, J. E. Moser, M. Grätzel, N.-G. Park *Sci. Rep.* **2012**, 2, 591.
[10] M. M. Lee, J. Teuscher, T. Miyasaka, T. N. Murakami, H. J. Snaith *Science*. **2012**, 338, 643-647.
[11] NREL_chart, https://www.nrel.gov/pv/cell-efficiency.html.
[12] Y. Chen, A. K. Athienitis, K. Galal *Solar Energy*. **2010**, 84, 1892-1907.
[13] C. Ballif, L.-E. Perret-Aebi, S. Lufkin, E. Rey *Nat Energy.* **2018**, 3, 438-442.
[14] Y. Ke, C. Zhou, Y. Zhou, S. Wang, S. H. Chan, Y. Long *Adv. Funct. Mater.* **2018**, 28, 1800113.
[15] H. S. Jung, G. S. Han, N.-G. Park, M. J. Ko *Joule*. **2019**, 3, 1850-1880.
[16] Q. Tai, F. Yan *Adv. Mater.* **2017**, 29, 1700192.
[17] Q. Xue, R. Xia, C. J. Brabec, H.-L. Yip *Energy Environ. Sci.* **2018**, 11, 1688-1709.
[18] J. Sun, J. J. Jasieniak *J. Phys. D: Appl. Phys.* **2017**, 50, 093001.
[19] A. A. F. Husain, W. Z. W. Hasan, S. Shafie, M. N. Hamidon, S. S. Pandey *Renew Sustain Energy Rev.* **2018**, 94, 779-791.
[20] B. Shi, L. Duan, Y. Zhao, J. Luo, X. Zhang *Adv. Mater.* **2020**, 32, 1806474.
[21] G. Y. Yoo, R. Azmi, C. Kim, W. Kim, B. K. Min, S.-Y. Jang, Y. R. Do *ACS Nano*. **2019**, 13, 10129-10139.
[22] A. Cannavale, G. E. Eperon, P. Cossari, A. Abate, H. J. Snaith, G. Gigli *Energy Environ. Sci.* **2015**, 8, 1578-1584.
[23] Y. Xia, X. Liang, Y. Jiang, S. Wang, Y. Qi, Y. Liu, L. Yu, H. Yang, X.-Z. Zhao *Adv. Energy Mater.* **2019**, 9, 1900720.
[24] K. M. Boopathi, C. Hanmandlu, A. Singh, Y.-F. Chen, C. S. Lai, C. W. Chu *ACS Appl. Energy Mater.* **2018**, 1, 632-637.
[25] X. Xia, Z. Ku, D. Zhou, Y. Zhong, Y. Zhang, Y. Wang, M. J. Huang, J. Tu, H. J. Fan *Mater. Horiz.* **2016**, 3, 588-595.
[26] F. Zhou, Z. Ren, Y. Zhao, X. Shen, A. Wang, Y. Y. Li, C. Surya, Y. Chai *ACS Nano*. **2016**, 10, 5900-5908.
[27] J. Sun, Y. Li, J. Sun, Z. Zhu, Y. Zhai, S. Dong *Chem. Commun.* **2019**, 55, 12060-12063.
[28] L. M. Wheeler, D. T. Moore, R. Ihly, N. J. Stanton, E. M. Miller, R. C. Tenent, J. L. Blackburn, N. R. Neale *Nat Commun.* **2017**, 8, 1722.
[29] M. De Bastiani, M. I. Saidaminov, I. Dursun, L. Sinatra, W. Peng, U. Buttner, O. F. Mohammed, O. M. Bakr *Chem. Mater.* **2017**, 29, 3367-3370.
[30] J. Lin, M. Lai, L. Dou, C. S. Kley, H. Chen, F. Peng, J. Sun, D. Lu, S. A. Hawks, C. Xie, F. Cui, A. P. Alivisatos, D. T. Limmer, P. Yang *Nat Mater.* **2018**, 17, 261-267.
[31] Y. Zhang, C. Y. Tso, J. S. Iñigo, S. Liu, H. Miyazaki, C. Y. H. Chao, K. M. Yu *Applied Energy*. **2019**, 254, 113690.
[32] R. F. Service *Science*. **2018**, doi:10.1126/science.aat0827.
[33] ViaSolis, https://www.youtube.com/watch?v=LXlnT-hhFfg.
[34] Y. Guo, K. Shoyama, W. Sato, E. Nakamura *Adv. Energy Mater.* **2016**, 6, 1502317.
[35] T. Bu, S. Shi, J. Li, Y. Liu, J. Shi, L. Chen, X. Liu, J. Qiu, Z. Ku, Y. Peng, J. Zhong, Y.-B. Cheng, F. Huang *ACS Appl. Mater. Interfaces.* **2018**, 10, 14922-14929.
[36] D. Bi, W. Tress, M. I. Dar, P. Gao, J. Luo, C. Renevier, K. Schenk, A. Abate, F. Giordano, J.-P. Correa Baena, J.-D. Decoppet, S. M. Zakeeruddin, M. K. Nazeeruddin, M. Grätzel, A. Hagfeldt *Science Advances*. **2016**, 2, e1501170.
[37] D. Yang, R. Yang, K. Wang, C. Wu, X. Zhu, J. Feng, X. Ren, G. Fang, S. Priya, S. Liu *Nat. Commun.* **2018**, 9, 3239.
[38] C. Wu, K. Wang, M. Batmunkh, A. S. R. Bati, D. Yang, Y. Jiang, Y. Hou, J. G. Shapter, S. Priya *Nano Energy*. **2020**, 70, 104480.
[39] C. Roldán-Carmona, O. Malinkiewicz, R. Betancur, G. Longo, C. Momblona, F. Jaramillo, L. Camacho, H. J. Bolink *Energy Environ. Sci.* **2014**, 7, 2968-2973.

[40] L. K. Ono, S. Wang, Y. Kato, S. R. Raga, Y. Qi *Energy Environ. Sci.* **2014**, 7, 3989-3993.
[41] P. You, Z. Liu, Q. Tai, S. Liu, F. Yan *Adv. Mater.* **2015**, 27, 3632-3638.
[42] J. W. Jung, C.-C. Chueh, A. K.-Y. Jen *Adv. Energy Mater.* **2015**, 5, 1500486.
[43] G. E. Eperon, V. M. Burlakov, A. Goriely, H. J. Snaith *ACS Nano*. **2014**, 8, 591-598.
[44] G. E. Eperon, D. Bryant, J. Troughton, S. D. Stranks, M. B. Johnston, T. Watson, D. A. Worsley, H. J. Snaith *J. Phys. Chem. Lett.* **2015**, 6, 129-138.
[45] M. T. Hörantner, P. K. Nayak, S. Mukhopadhyay, K. Wojciechowski, C. Beck, D. McMeekin, B. Kamino, G. E. Eperon, H. J. Snaith *Adv. Mater. Interfaces.* **2016**, 3, 1500837.
[46] J. H. Heo, M. H. Jang, M. H. Lee, H. J. Han, M. G. Kang, M. L. Lee, S. H. Im *J. Mater. Chem. A.* **2016**, 4, 16324-16329.
[47] M. T. Hörantner, W. Zhang, M. Saliba, K. Wojciechowski, H. J. Snaith *Energy Environ. Sci.* **2015**, 8, 2041-2047.
[48] S. Aharon, M. Layani, B.-E. Cohen, E. Shukrun, S. Magdassi, L. Etgar *Adv. Mater. Interfaces.* **2015**, 2, 1500118.
[49] H.-C. Kwon, A. Kim, H. Lee, D. Lee, S. Jeong, J. Moon *Adv. Energy Mater.* **2016**, 6, 1601055.
[50] E. Della Gaspera, Y. Peng, Q. Hou, L. Spiccia, U. Bach, J. J. Jasieniak, Y.-B. Cheng *Nano Energy*. **2015**, 13, 249-257.
[51] I. Jeon, J. Yoon, U. Kim, C. Lee, R. Xiang, A. Shawky, J. Xi, J. Byeon, H. M. Lee, M. Choi, S. Maruyama, Y. Matsuo *Adv. Energy Mater.* **2019**, 9, 1901204.
[52] F. R. Li, Y. Xu, W. Chen, S. H. Xie, J. Y. Li *J. Mater. Chem. A.* **2017**, 5, 10374-10379.
[53] M. Batmunkh, C. J. Shearer, M. J. Biggs, J. G. Shapter *J. Mater. Chem. A.* **2015**, 3, 9020-9031.
[54] C. Zhang, S. Wang, H. Zhang, Y. Feng, W. Tian, Y. Yan, J. Bian, Y. Wang, S. Jin, S. M. Zakeeruddin, M. Grätzel, Y. Shi *Energy Environ. Sci.* **2019**, 12, 3585-3594.
[55] J. Cao, F. Meng, L. Gao, S. Yang, Y. Yan, N. Wang, A. Liu, Y. Li, T. Ma *RSC Adv.* **2019**, 9, 34152-34157.
[56] C. Zhang, B. Anasori, A. Seral-Ascaso, S.-H. Park, N. McEvoy, A. Shmeliov, G. S. Duesberg, J. N. Coleman, Y. Gogotsi, V. Nicolosi *Adv. Mater.* **2017**, 29, 1702678.
[57] L. Yu, A. S. R. Bati, T. S. L. Grace, M. Batmunkh, J. G. Shapter *Adv. Energy Mater.* **2019**, 9, 1901063.
[58] A. Cannavale, M. Hörantner, G. E. Eperon, H. J. Snaith, F. Fiorito, U. Ayr, F. Martellotta *Applied Energy*. **2017**, 194, 94-107.
[59] N. J. Jeon, J. H. Noh, W. S. Yang, Y. C. Kim, S. Ryu, J. Seo, S. I. Seok *Nature*. **2015**, 517, 476-480.
[60] J. H. Noh, S. H. Im, J. H. Heo, T. N. Mandal, S. I. Seok *Nano Lett.* **2013**, 13, 1764-1769.
[61] T. Jesper Jacobsson, J.-P. Correa-Baena, M. Pazoki, M. Saliba, K. Schenk, M. Grätzel, A. Hagfeldt *Energy Environ. Sci.* **2016**, 9, 1706-1724.
[62] W. Zhang, M. Anaya, G. Lozano, M. E. Calvo, M. B. Johnston, H. Míguez, H. J. Snaith *Nano Lett.* **2015**, 15, 1698-1702.
[63] Y. Deng, Q. Wang, Y. Yuan, J. Huang *Mater. Horiz.* **2015**, 2, 578-583.
[64] K.-T. Lee, M. Fukuda, S. Joglekar, L. J. Guo *J. Mater. Chem. C.* **2015**, 3, 5377-5382.
[65] J.-H. Lu, Y.-L. Yu, S.-R. Chuang, C.-H. Yeh, C.-P. Chen *J. Phys. Chem. C.* **2016**, 120, 4233-4239.
[66] C. O. Ramírez Quiroz, C. Bronnbauer, I. Levchuk, Y. Hou, C. J. Brabec, K. Forberich *ACS Nano*. **2016**, 10, 5104-5112.
[67] Y. Jiang, B. Luo, F. Jiang, F. Jiang, C. Fuentes-Hernandez, T. Liu, L. Mao, S. Xiong, Z. Li, T. Wang, B. Kippelen, Y. Zhou *Nano Lett.* **2016**, 16, 7829-7835.
[68] Y. Gao, H. Luo, Z. Zhang, L. Kang, Z. Chen, J. Du, M. Kanehira, C. Cao *Nano Energy*. **2012**, 1, 221-246.

[69] M. Wang, X. Xing, I. F. Perepichka, Y. Shi, D. Zhou, P. Wu, H. Meng *Adv. Energy Mater.* **2019**, 9, 1900433.
[70] C. Bechinger, S. Ferrere, A. Zaban, J. Sprague, B. A. Gregg *Nature*. **1996**, 383, 608-610.
[71] C. G. Granqvist, P. C. Lansåker, N. R. Mlyuka, G. A. Niklasson, E. Avendaño *Sol. Energy Mater. Sol. Cells.* **2009**, 93, 2032-2039.
[72] Y. Wang, E. L. Runnerstrom, D. J. Milliron *Annu. Rev. Chem. Biomol. Eng.* **2016**, 7, 283-304.
[73] H.-K. Kwon, K.-T. Lee, K. Hur, S. H. Moon, M. M. Quasim, T. D. Wilkinson, J.-Y. Han, H. Ko, I.-K. Han, B. Park, B. K. Min, B.-K. Ju, S. M. Morris, R. H. Friend, D.-H. Ko *Adv. Energy Mater.* **2015**, 5, 1401347.
[74] F. Favoino, F. Fiorito, A. Cannavale, G. Ranzi, M. Overend *Applied Energy*. **2016**, 178, 943-961.
[75] A. Cannavale, M. Manca, F. Malara, L. De Marco, R. Cingolani, G. Gigli *Energy Environ. Sci.* **2011**, 4, 2567-2574.
[76] J.-J. Wu, M.-D. Hsieh, W.-P. Liao, W.-T. Wu, J.-S. Chen *ACS Nano*. **2009**, 3, 2297-2303.
[77] W. Ning, X.-G. Zhao, J. Klarbring, S. Bai, F. Ji, F. Wang, S. I. Simak, Y. Tao, X.-M. Ren, L. Zhang, W. Huang, I. A. Abrikosov, F. Gao *Adv. Funct. Mater.* **2019**, 29, 1807375.
[78] M. Batmunkh, C. J. Shearer, M. J. Biggs, J. G. Shapter *J. Mater. Chem. A.* **2016**, 4, 2605-2616.
[79] P.-C. Hsu, S. Wang, H. Wu, V. K. Narasimhan, D. Kong, H. Ryoung Lee, Y. Cui *Nat. Commun.* **2013**, 4, 2522.
[80] L. Yu, C. Shearer, J. Shapter *Chem. Rev.* **2016**, 116, 13413-13453.
[81] Y. Ma, L. Zhi *Small Methods*. **2019**, 3, 1800199.

((**For Essays, Feature Articles, Progress Reports, and Reviews,** please insert up to three author biographies and photographs here, max. 100 words each))

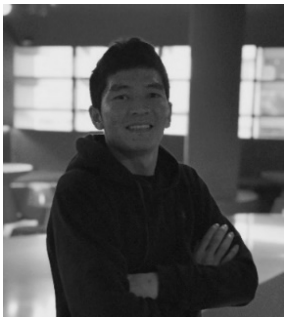

Munkhbayar Batmunkh is a research fellow in Centre for Clean Environment and Energy at Griffith University, Australia. He also worked at the University of Queensland (2018-2019) and Flinders University (2017-2018), and was a visiting scholar in Virginia Tech in the USA. He received his Ph.D. in chemical engineering in 2017 from the University of Adelaide (Australia). He obtained his 'Master of Engineering' degree in 2012 from Gyeongsang National University, in South Korea, and 'Bachelor of Science' degree in 2010 at the National University of Mongolia, in Mongolia. His research interests focus on the production of functional nanomaterials (e.g. nanocarbons and 2D materials) for energy related applications such as solar cells and catalysis.

Yu Lin Zhong completed his PhD in Chemistry at National University of Singapore and did his post-doctoral training at Princeton University (2009) and Massachusetts Institute of Technology (2011). Thereafter, he worked as a Research Scientist at Institute of Bioengineering and Nanotechnology, A*STAR Singapore, (2012) and an ARC DECRA Fellow at Monash University (2013). He joined Griffith University in 2016 and is currently an Associate Professor at the School of Environment and Science (ESC) and Centre for Clean Environment and Energy (CCEE). His research group interests include electrochemical production of 2D nanomaterials, 3D printing, smart windows and wearable devices.

Huijun Zhao obtained his PhD in Chemistry in 1994 from the University of Wollongong, Australia. He currently holds a profesorial position at Griffith University and is the founding Director of Griffith University's Centre for Clean Environment and Energy. He is a Fellow of Royal Society of Chemistry (FRSC) and Fellow of the Royal Australian Chemical Institute (FRACI), and the recipient of The R.H. Stokes Medal for electrochemistry. He has expertise in energy and environmental nanomaterials. One of his current pursuits is to explore new means to utilize nonprecious materials for energy and environmental applications.

The advances being achieved in the perovskite materials based building-integrated photovoltaics for four areas of applications, namely semitransparent windows, colorful wall facades, electrochromic windows and thermochromic windows, are presented. Critical roadmaps on future developments of this cutting-edge research field are provided.

Keyword: Perovskites for Building Integrations

Munkhbayar Batmunkh, Yu Lin Zhong* and Huijun Zhao*

Title: Recent Advances in Perovskites-based Building-Integrated Photovoltaics